Design and self-assembly of two-dimensional DNA crystals

Erik Winfree*, **Furong Liu**†, **Lisa A. Wenzler**† & **Nadrian C. Seeman**†

* *Computation and Neural Systems, California Institute of Technology, Pasadena, California 91125, USA*
† *Department of Chemistry, New York University, New York, New York 10003, USA*

Molecular self-assembly presents a 'bottom-up' approach to the fabrication of objects specified with nanometre precision. DNA molecular structures and intermolecular interactions are particularly amenable to the design and synthesis of complex molecular objects. We report the design and observation of two-dimensional crystalline forms of DNA that self-assemble from synthetic DNA double-crossover molecules. Intermolecular interactions between the structural units are programmed by the design of 'sticky ends' that associate according to Watson–Crick complementarity, enabling us to create specific periodic patterns on the nanometre scale. The patterned crystals have been visualized by atomic force microscopy.

Control of the detailed structure of matter on the finest possible scale is a major goal of chemistry, materials science and nanotechnology. This goal may be approached in two steps: first, the construction of individual molecules through synthetic chemistry; and second, the arrangement of molecular building blocks into larger structures. The simplest arrangements of molecular units, in two or three dimensions, are periodic—a crystal. Design components for crystals must have definable intermolecular interactions and must be rigid enough to prevent the formation of ill-defined aggregates[1]. Branched DNA molecules with sticky ends are promising for macro-molecular crystal design[2] because their intermolecular interactions can be programmed through sticky ends[3] that associate to produce B-form DNA[4]; however, studies of three- and four-arm junctions reveal that the angles flanking their branchpoints are flexible[5,6].

The need for a rigid design component with predictable and controllable interactions has led to the utilization of the antiparallel DNA double-crossover motif[7] for this purpose. Double-crossover (DX) molecules are analogues of intermediates in meiosis[8] that consist of two side-by-side double-stranded helices linked at two crossover junctions. Antiparallel DX molecules have a rigidity that is lacking in conventional branched junctions, indicating that they might be suitable for use in the assembly of periodic matter[9].

These findings stimulated a theoretical proposal to use two-dimensional (2-D) lattices of DX molecules[10] for DNA-based computation[11]. In the mathematical theory of tilings[12], rectangular tiles with programmable interactions, known as Wang tiles, can be designed so that their assembly must mimic the operation of a chosen Turing Machine[13]. DX molecules acting as molecular Wang tiles could self-assemble to perform desired computations[10,14,15]. Consequently, the ability to create 2-D lattices of DX molecules assumes additional interest as a step towards the design of molecular algorithms.

Here we report the assembly, from DX molecules, of three 2-D lattices with two distinct topologies. The DX molecules, $\sim 2 \times 4 \times 13$ or $2 \times 4 \times 16$ nm in size, self-assemble in solution to form single-domain crystals as large as 2×8 μm with uniform thickness between 1 and 2 nm, as visualized by atomic force microscopy[16] (AFM). By incorporating a DNA hairpin into a DX molecule to serve as a topographic label, we have produced stripes above the surface at intervals of 25, 32 and 64 nm. Two-component lattices have been assembled with a stripe every other unit; by programming sticky-ended associations differently, four-component lattices have been produced with a strip every fourth unit. This observation demonstrates that it is possible to create specific lattices with programmable structures and features on a nanometre scale.

Design of DNA crystal

Our approach to two-dimensional crystal design is derived from the mathematical theory of tiling[10,12]. The desired lattice is specified by a set of Wang tiles with coloured edges; the Wang tiles may be placed next to each other only if their edges are identically coloured where they touch (Fig. 1a). Our goal is to design synthetic molecular units corresponding to these tiles, such that they will self-assemble into a crystal that obeys the colouring conditions. As an initial demonstration of molecular Wang tiles, we have chosen the simplest non-trivial set of tiles: two tiles, **A** and **B**, which make a striped lattice (Fig. 1a, left). We also demonstrate a set of four tiles that produce a striped lattice with a greater period (Fig. 1a, right). Translated into molecular terms, we obtain DX systems that self-assemble in solution into two-dimensional crystals with a well defined subunit structure.

The antiparallel DX motif[7] consists of two juxtaposed immobile 4-arm junctions[2] arranged so that at each junction the non-crossover strands are antiparallel to each other. There are five distinct DX motifs, but only two are stable in small molecules[7]: these are called DAO (double crossover, antiparallel, odd spacing) and DAE (double crossover, antiparallel, even spacing). The design depends critically upon the twist of the B-form DNA double helix, in which a full turn takes place in ~ 10.5 base pairs[17,18]. DAO molecules have an odd number of half-turns (e.g. 3 half-turns is ~ 16 base pairs) between the crossover points, whereas DAE molecules have an even number of half-turns (for example, 4 half-turns is ~ 21 base pairs). Computer models of the DX molecules used in this study are shown in Fig. 1b. The DAO molecules consist of four strands of DNA, each of which participates in both helices. The DAE molecules consist of three strands that participate in both helices (yellow, light blue, green), and two strands that do not cross over (red, dark blue). Each corner of each DX unit has a single-stranded sticky end with a unique sequence; specific association of DX units is controlled by choosing sticky ends with Watson–Crick complementarity.

To ensure that the component strands form the desired complexes, strand sequences must be designed carefully so that alternative associations and conformations are unlikely. Therefore we must solve the 'negative design problem'[19–21] for DNA: find sequences that maximize the free energy difference between the desired conformation and all other possible conformations. We use the heuristic principle of sequence symmetry minimization[2,19] to minimize the length and number of unintentional Watson–Crick

complementary subsequences. In each DX molecule's sequences, there are no 6-base subsequences complementary to other 6-base subsequences except as required by the design, and spurious 5-base complementarity is rare. Thus it is expected that during self-assembly, the DNA strands spend little time in undesired associations and form DX units with high yield.

DX units can be designed that will fit together into a two-dimensional crystalline lattice. Here we use either two or four distinct unit types (Fig. 1a) to produce striped lattices. We use two separate systems to implement the two-unit lattice, one consisting of two DAO units, the other consisting of two DAE units. The

lattices produced by these systems are called DAO-E and DAE-O, respectively, to indicate the number of half-turns between crossover points on adjacent units; their distinct topologies are shown in Fig. 1c. Covalently joining adjacent nucleotides at nicks in the lattice, by chemical or enzymatic ligation, would result in a 'woven fabric' of DNA strands. Ligation of the DAO-E design produces four distinct strand types, each of which continues infinitely in the vertical direction (here, the terms 'vertical' and 'horizontal' will always be as in Fig. 1c). The DAE-O design involves two small nicked circular strands in addition to four infinite strands, two of which extend horizontally and two of which extend vertically. The DAO-E
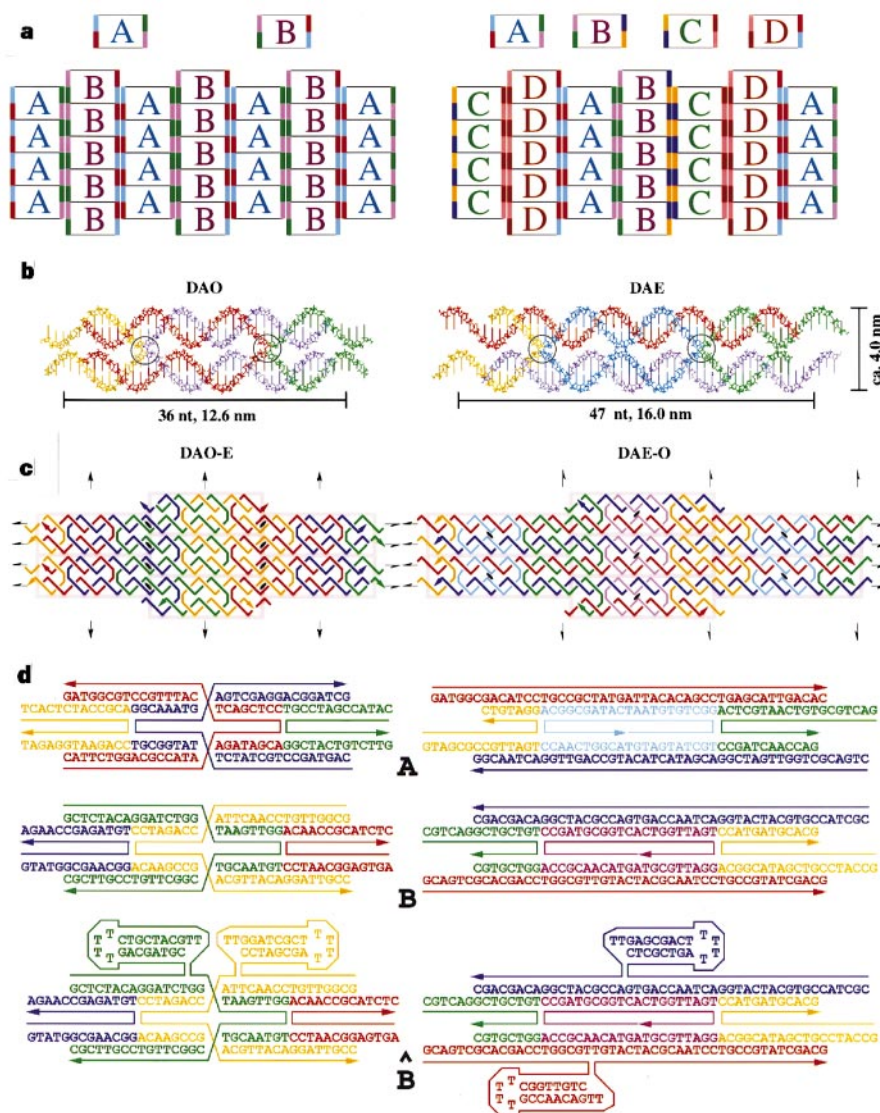
Figure 1 Design of DX molecular structure and arrangement into 2-D lattices. **a**, The logical structure for 2-D lattices consisting of two units and four units. In the two-unit design, type **A** units have four coloured edge regions, each of which match exactly one coloured region of the adjacent type **B** units. Similarly, in the four-unit design, the edge colours are chosen uniquely to define the desired relations between neighbouring tiles. Note that rotations and reflections of Wang tiles are disallowed; an equivalent restriction could also be obtained by using non-rectangular tiles or more complex patterns of colours. **b**, Model structures for DAO and DAE type **A** units. Each component oligonucleotide is shown in a unique colour. The crossover points are circled. Complete base stacking at the crossover points is assumed. Computer models showing every nucleotide (nt) were generated using NAMOT2 (ref. 39). **c**, The lattice topologies produced by the DAO and DAE units. Each DX unit is highlighted by a grey rectangle. A unique colour is chosen for each strand type which would be formed after covalent ligation of units. Arrowheads indicate the 3′ ends of strands. Black ellipses indicate dyad symmetry axes perpendicular to the plane; black arrows indicate dyad axes in the plane (full arrowhead) or screw axes (half arrowhead). The symmetries of the DAO-E and DAE-O lattices are those corresponding to the layer groups[40] $P2_122$ and $P2_12_12$ respectively. The boundaries of the DAE-O units are not designed to coincide with the vertical symmetry elements. **d**, The actual sequences used in the reported experiments (see Methods for several exceptions). The schematics accurately report primary and secondary structure–oligonucleotide sequence and paired bases–but are not geometrically or topologically faithful because they do not show the double-helical twist. Both type **B** and type **B̂** are shown, indicating where the hairpin sequences are inserted. Note that for each type–**A**, **B**, and **B̂**–there is both a DAO unit and a DAE unit.

design has the advantage of using simple 4-strand DX units, whereas in the DAE-O design, the horizontal and vertical strands can serve as reporters for the extent of self-assembly if the molecules are ligated and analysed by gel electrophoresis. We have investigated both the DAO-E and DAE-O systems in parallel to show that the same principles of self-assembly govern both systems. Therefore, except where noted, our discussion will apply to both systems.

Control of self-assembly to yield the 2-D lattice is obtained by two design criteria. First, the sticky-end sequences for each desired contact are unique; this ensures that the orientations and adjacency relations of the DX units comply exactly with the design in Fig. 1a. Sticky ends are lengths 5 and 6 for the DAO-E and DAE-O designs respectively, so that each correct contact contributes ~8 or 14 kcal mol^{-1} to the free energy of association at 25 °C, according to a nearest-neighbour model[22]. Second, the lengths of the DX arms and sticky ends, and thus the separations between crossover points, respect as closely as possible the natural twist of the B-form DNA double helix; thus adjacent DX molecules are effectively coupled by torsional springs whose equilibrium positions have been designed to keep the adjacent DX molecules coplanar. For example, a linear rather than planar polymer could result if each unit makes two sticky-end bonds to each neighbouring unit, but this would require overtwisting, undertwisting, or bending of the double helix, and thus is discouraged by our design.

Figure 1d shows the DX units and sequences used in our experiments, except as noted in Methods. In each system, there are two fundamental DX units, called **A** and **B**, and, additionally, an alternative form **B̂** that contains two hairpin-terminated bulged 3-arm junctions (similar to the DX + J motif[9]). On the basis of studies of bulged 3-arm junctions[23], we expect that in each unit, one hairpin will point up and out of the plane of the DX crystal, while the other hairpin will point down and into the plane, without significantly affecting the rigidity of the molecule[9]. The **B̂** units will replace the **B** units and serve as contrast agents for AFM imaging, because their increased height can be measured directly. Related sequences were used for the four-unit lattice **ABCD̂** and for studies involving gold labelling or alternative placements of the hairpins.

Characterization by gel electrophoresis

A prerequisite for lattice self-assembly is the formation of the DX units from their component strands. A thorough investigation of this issue was done for the original studies of DX[7]; that the new designs also behave well constitutes further validation of the antiparallel DX motif. Because the sticky ends of **A** units have affinity only for sticky ends of **B** units, and not for themselves, neither **A** nor **B** alone in solution can assemble into a lattice. Thus the formation of isolated DX units can be monitored easily by non-denaturing gel electrophoresis, as described previously[7], and more than 95% of the material is seen in the expected band.

Solutions containing **A** units and **B** units can be mixed and annealed to form **AB** lattices. Enzymatic ligation of these lattices with T4 DNA ligase should produce long covalent DNA strands. The nicks, where strands from adjacent DX units abut, are all on the upper or lower surface of the lattice, where they are accessible to the enzyme. The long strands can serve as reporters of successful lattice formation; shorter strands report either the presence of small aggregates or an occasional failure to ligate within the lattice. In the DAO-E design there are four vertical reporter strands, whereas in the DAE-O design there are two horizontal and two vertical reporter strands. All four reporter strands extend for more than 30 repeats when visualized by denaturing polyacrylamide gel electrophoresis (PAGE) (Fig. 2; data for DAO-E not shown). Longer strands co-migrate on this gel, so we cannot determine the full extent of polymerization. These results suggest that the lattice is a good substrate for T4 DNA ligase, and that the lattice can form with more than 30×30 units. However, unintended associations or side

reactions could lead to similar distributions of strand lengths after ligation. Direct physical observation is necessary to confirm lattice assembly.

AFM imaging

We have used atomic force microscopy[16] to demonstrate unequivocally the formation of 2-D lattices. **A** and **B** units are annealed separately, then combined and annealed together to form **AB** lattices. The resulting solution is deposited for adsorption on an atomically flat mica surface, and then imaged under isopropanol by contact mode AFM[24]. The solution is not treated with DNA ligase, and thus the lattices are held together only by noncovalent interactions (for example, hydrogen bonds and base stacking). This protocol ensures that the solution contains no protein contaminants and demonstrates that ligase activity is not necessary for the self-assembly process. Negative controls of buffer alone and of **A** or **B** alone show no aggregates larger than 20 nm (data not shown). In separate experiments, **A** and **B** DAO units were modified by the removal of two sticky ends from each unit (for example, all yellow and red sticky ends in Fig. 1d); when the modified **A** and **B** units were annealed together, we observed only linear and branched structures with apparent widths typically less than 10 nm (data not shown), providing additional negative controls. However, the unmodified **AB**
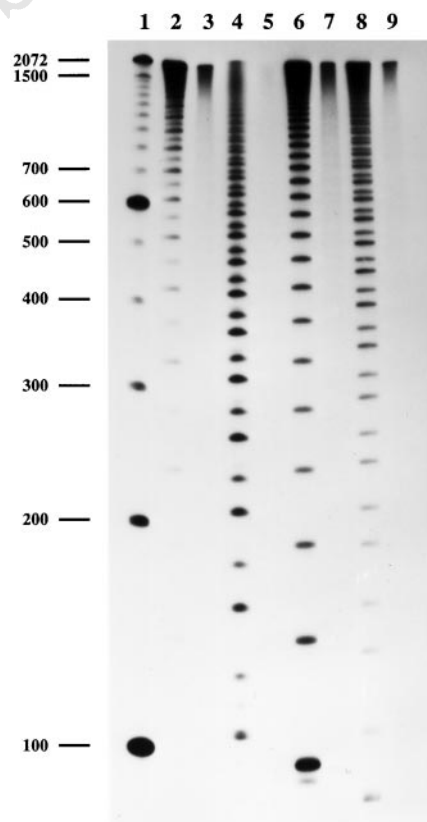

Figure 2 Autoradiogram of a 4% denaturing polyacrylamide gel showing the product after assembly of 2-D lattice DAE-O (**AB**), ligation to form long covalent strands, and denaturing to separate the strands. Lane 1 contains a ladder or markers at 100-base intervals. In the remaining lanes, a different strand from unit **B** is labelled: lanes 2 and 3 correspond to red strands (Fig. 1c, right), lanes 4 and 5 are green strands, lane 6 and 7 are blue strands, and lanes 8 and 9 are yellow strands. *Escherichia coli* exonucleases I and III were added to the material in the odd-numbered lanes to degrade single-stranded species, indicating that no circular products were formed. As red strands are lengths 46 and 48, in lane 2 we see bands at lengths $94k$ and $94k + 48$ for integers k; green strands are lengths 31 and 21, so lane 4 has bands at $52k$ and $52k + 21$; blue strands are both length 47, so lane 6 has bands at $94k$ and $94k + 47$; and yellow strands are lengths 21 and 31, so lane 8 has bands at $52k$ and $52k + 31$.

samples contain 2-D sheets many micrometres long, often more than 200 nm wide (Fig. 3a, d). The apparent height of the sheets is 1.4 ± 0.5 nm, suggestive of a monolayer of DNA. The sheets often seem ripped and appear to have a grain, in that rips have a preferred direction consistent with the design (Fig. 1c). In the DAO-E lattice, a vertical rip requires breaking six sticky-end bonds per 12 nm torn, whereas a horizontal rip requires breaking only one sticky-end bond per 13 nm torn. A possible vertical column, perpendicular to the rips, is indicated in Fig. 3a (arrows). Although in this image the columns are barely perceptible, Fourier analysis shows a peak at 13 ± 1 nm, suggesting that observed columns are 1 DX wide. Periodic topographic features would not be expected in the ideal **AB** lattice; however, a vertically stretched lattice may have gaps between the DX units that could produce the periodic features seen here. Because crystals are found in AFM samples taken from both the top and the bottom of the solution, we believe that crystals form in solution and are not due to interaction with a surface.

Control of surface topography

The self-assembling **AB** lattice can serve as scaffolding for other molecular structures. We have decorated **B** with two DNA hairpin sequences inserted into its component strands, which we call **B̂** (Fig. 1d). So decorated, the vertical columns of the lattice become strikingly apparent as stripes in AFM images (Fig. 3b, c, e, f), further confirming the proper self-assembly of the 2-D lattice. The spacing of the decorated columns is 25 ± 2 nm for the DAO-E lattice and 33 ± 3 nm for the DAE-O lattice, indicating that every other column is decorated, in accord with the design. Slow annealing at 20 °C and gentle handling of the DAO-E sample during deposition and washing has produced single crystals measuring up to 2 × 8 μm (Fig. 4a–c). Close examination shows that the stripes are continuous across the crystal, and thus it appears to be a single domain containing over 500,000 DX units.

Instead of DNA hairpins, other chemical groups can be used to label the DX molecules. Previously, biotin–streptavidin–gold has been used to label linear DNA for imaging by AFM[25,26]. We have used 1.4-nm nanogold–streptavidin conjugates to label DAE molecules. For these experiments, the central strand of **B** contains a 5′ biotin group; after assembly of **AB** lattices, the solution containing DNA lattices is incubated with streptavidin–nanogold conjugates and
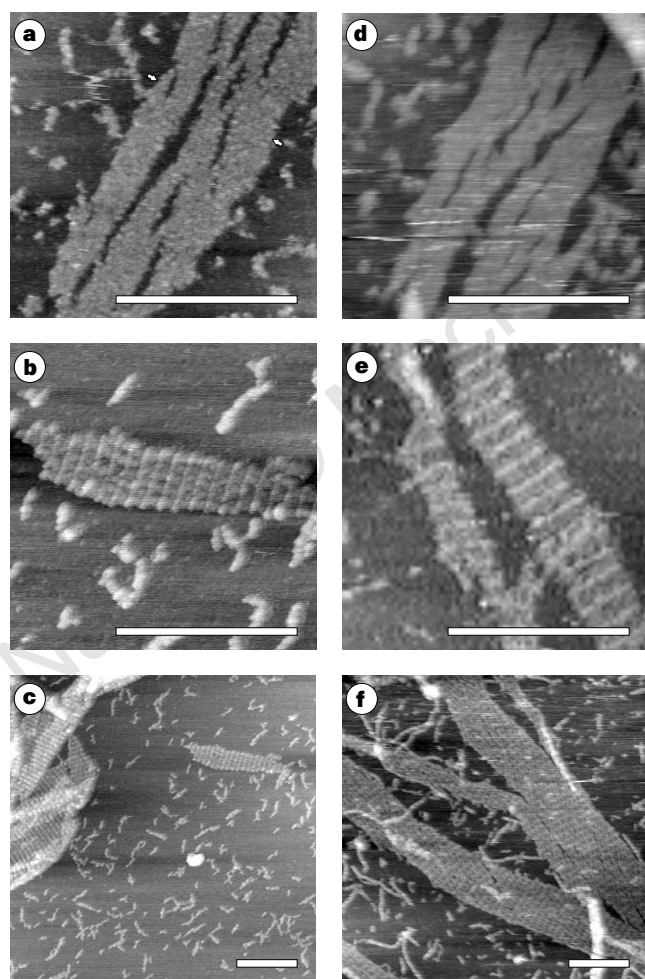

Figure 3 AFM images of two-unit lattices. **a**, DAO-E **AB** lattice. A possible vertical column is indicated by the arrows. Fourier analysis shows 13 ± 1 nm periodicity; each DAO is 12.6 nm wide. **b** and **c**, DAO-E **AB̂** lattice (two views of the same sample). Stripes have 25 ± 2 nm periodicity; the expected value is 25.2 nm. **d**, DAE-O **AB** lattice. **e** and **f**, DAE-O **AB̂** lattice (for different samples, see Methods). Stripes have 33 ± 3 nm periodicity; the expected value is 32 nm. All scale bars are 300 nm; images show 500 × 500 nm or 1.5 × 1.5 μm. The grey scale indicates the height above the mica surface; the apparent lattice height is between 1 and 2 nm.
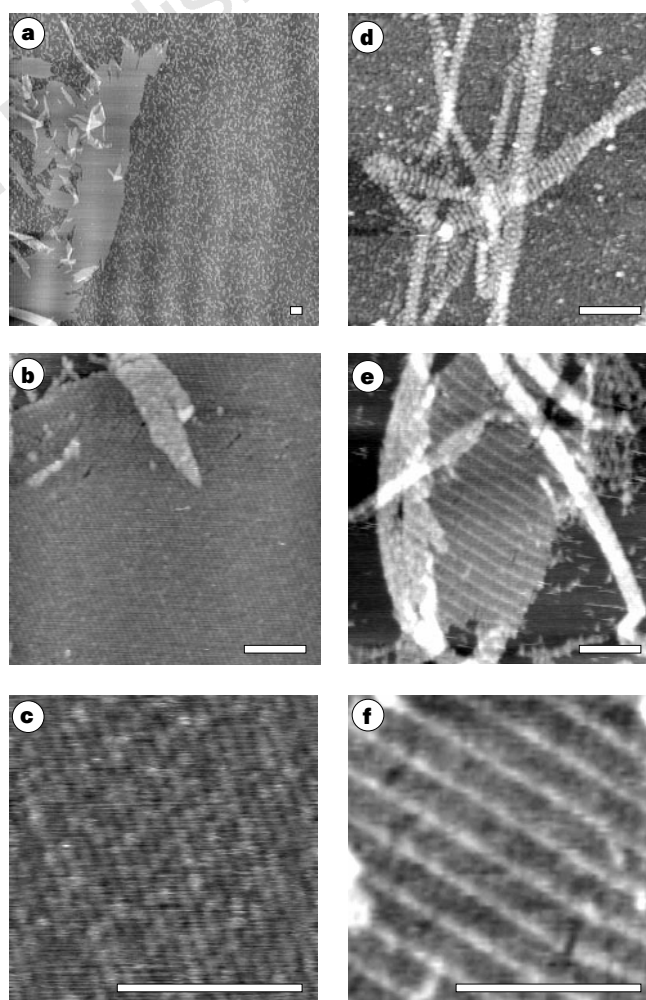
Figure 4 AFM images showing large crystals and modifications of lattice periodicity and surface features. **a–c**, DAO-E **AB̂** lattice at three levels of detail (all the same sample). The largest domain is ~2 × 8 μm, and contains ~500,000 DX units. **d**, DAE-O **AB** lattice in which **B** has been labelled with biotin–streptavidin–nanogold. **e** and **f**, DAE-O **ABCD̂** lattice at two levels of detail (the same sample). Stripes have 66 ± 5 nm periodicity; the expected value is 64 nm. All scale bars are 300 nm; images show 500 × 500 nm, 1.5 × 1.5 μm, or 10 × 10 μm. The grey scale indicates the height above the mica surface; the apparent lattice height is between 1 and 2 nm.

then imaged by AFM (Fig. 4d). We have not confirmed that the nanogold particles remain conjugated to the streptavidin molecules; the surface topography may be due to streptavidin molecules alone.

We have also tested DAO and DAE systems incorporating only one of the two hairpins in $\hat{\mathbf{B}}$, DAO systems in which the 3-arm junctions are relocated by two nucleotides towards the centre of the molecule, and DAE systems in which the arms are one nucleotide longer or shorter. All systems produced results similar to those shown in Fig. 3 when imaged by AFM (data not shown). The lattice assembly appears to be robust to variations in the local DX structure and is not sensitive to small variations in the annealing protocol. (The results reported here were obtained in two laboratories using different buffers, annealing conditions, and AFM instruments.)

Choice of sticky ends predictably determines the associations between DX units. Therefore it is straightforward to modify the **AB** system into a 4-DX system with twice the period (Fig. 1a, right). This requires the use of twice as many unique sticky-end sequences to control the unique association of DX units **A**, **B**, **C**, and **D**. We have created such a system in the DAE-O topology, where a single unit, $\hat{\mathbf{D}}$, is decorated with two hairpins. Crystals in this system show stripes spaced every 66 ± 5 nm, confirming that every fourth vertical column is decorated (Fig. 4e, f).

In all images of **AB**, **AB̂** and **ABCD̂** systems, we observed many DNA structures in addition to the isolated 2-D crystals discussed above. In many images, the 2-D crystals appear to overlap, leading to discrete steps in thickness (Figs 3c, 4a, d). The arrangement of crystals on the mica—solitary, overlapping, piled up like driftwood, ripped to shreds—depends sensitively upon DNA concentration and upon the sample preparation procedure, especially the wash step. Prominently, the background of every image contains small objects, which we assume to be associations of small numbers of DX units. Also, long, thin 'rods' appear in some preparations (Figs 3f, 4d, lower right). These structures have not been characterized.

Applications

Self-assembly is increasingly becoming recognized as a route to nanotechnology[27]. Our results demonstrate the potential of using DNA to create self-assembling periodic nanostructures. The periodic blocks used here are composed of either two or four individual DX units. However, the number of component tiles in the repeat unit does not appear to be limited to such small numbers, suggesting that complex patterns could be assembled into periodic arrays. These patterns could be either direct targets in nanofabrication or aids to the construction of such targets. Because oligonucleotide synthesis can readily incorporate modified bases at arbitrary positions, it should be possible to control the structure within the periodic block by decoration with chemical groups, catalysts, enzymes and other proteins[28], metallic nanoclusters[29,30], conducting silver clusters[31], DNA enzymes[32], or other DNA nanostructures such as polyhedra[33,34].

It may be possible to extend the two-dimensional lattices demonstrated here into three dimensions. Designed crystals could serve as scaffolds for the crystallization of macromolecules[2], as photonic materials with novel properties[35], as designable zeolite-like materials for use as catalysts or as molecular sieves[36], and as scaffolds for the assembly of molecular electronic components[37] or biochips[38].

The self-assembly of aperiodic structures should also be considered. It may be possible to design molecular Wang tiles that self-assemble into aperiodic crystals according to algorithmic rules[10,14]. It will be crucial to understand the mechanisms of crystallogenesis and crystal growth in this system to provide a firm underpinning for theoretical proposals of computation by self-assembly.

Progress in this field will require detailed knowledge of the physical, kinetic, structural, dynamic and thermodynamic parameters that characterize DNA self-assembly. Additionally, improved methods for error reduction and purification must be developed.

The approach described here provides a uniquely versatile experimental system for investigating these issues. □

Methods

DNA sequences and synthesis. Figure 1d shows sequences used in these experiments; for historical reasons, some figures show experiments where variants of these sequences were used. The sequences for DAO-E **A**, **B**, and **B̂** given in Fig. 1d were used for Fig. 3b, c. Figures 3a, 4a–c, show DAO systems with symmetrical sticky ends: the sequence for the green strands of DAO **A** is 5′TCACT…GAGAT3′ and the sequence for the blue strands of DAO **B** and **B̂** is 5′AGTGA…ATCTC3′. The sequences for the DAE-O **A** and **B** units used in Fig. 3d are modified from those given in Fig. 1d by deletion of the rightmost A·T base pair in the upper helix of **A**, addition of C to the upper-rightmost 5′ end of **A**, and deletion of C from the lower-leftmost 3′ end of **B**; also the central strand of **A** is cyclically permuted to begin 5′GCATGT… and the central strand of **B** is cyclically permuted to begin 5′GGTCAC…. For Fig. 3e, the sequences for the DAE-O **A** are as shown in Fig. 1d, but both hairpins of **B̂** stem from the lower helix; thus the upper strand is as in **B**, and the central strand is 5′ACTGGTT AGTGGATTGCGTAGGCGAGTAGTTTTCTACTCGCTTTACAACGCCACCG ATGCGGTC3′. The sequences for the DAE-O **A** and **B̂** units used in Fig. 3f are exactly as shown in Fig. 1d. Sequences for **ABCD̂** are available as Supplementary Information. All oligonucleotides were synthesized by standard methods, PAGE purified, and quantitated by ultraviolet absorption at 260 nm in H_2O.

Annealing of oligonucleotides. The strands of each DX unit were mixed stoichiometrically and dissolved to $0.2–2\,\mu M$ in TAE/Mg^{2+} buffer (40 mM Tris-HCl (pH 8.0), 1 mM EDTA, 3 mM Na^+, 12.5 mM Mg^{2+}) or in a HEPES buffer (10 mM HEPES, 6 mM $MgCl_2$, 1 mM EDTA, pH 7.8). The solutions were annealed from 90 °C to room temperature over the course of several hours in a Perkin-Elmer polymerase chain reaction (PCR) machine (to prevent concentration by evaporation) or were annealed from 100 °C to room temperature during 40 h in a 2-litre water bath insulated in a styrofoam box. To produce lattices, equal amounts of each DX were mixed and annealed from 50 °C to 20 °C for up to 36 h. In some cases (Fig. 3a–c), all strands were mixed together from the start.

Gel electrophoresis. For gel-based studies, T4 polynucleotide kinase (Amersham) was used to phosphorylate strands with ^{32}P; these strands were then PAGE-purified and mixed with an excess of unlabelled strands. Non-denaturing 4, 5, or 8% PAGE (19:1 acrylamide:bisacrylamide) in TAE/Mg^{2+} was done at 4 °C or at room temperature. For denaturing experiments, after annealing in T4 DNA ligase buffer (Amersham) (66 mM Tris-HCl (pH 7.6), 6.6 mM $MgCl_2$, 10 mM DTT, 66 μM ATP), 1 μl containing 10 units of T4 DNA ligase (Amersham) was added to 10 μl DNA solution and incubated for up to 24 h at 16 °C or at room temperature. For exonuclease reactions, 50 units of exonuclease III (Amersham) and 5 units of exonuclease I (Amersham) were added after ligation and incubated an additional 3.5 h at 37 °C. The solution was added to an excess of denaturing dye buffer (0.1% xylene cyanol FF tracking dye in 90% formamide with 1 mM EDTA, 10 mM NaOH) and heated to 90 °C for at least 5 min before loading. Denaturing gels contained 4% acrylamide (90:1 acrylamide:bisacrylamide) and 8.3 M urea in TBE (89 mM Tris-HCl (pH 8.0), 89 mM boric acid, 2 mM EDTA). Gels were analysed by using a Phosphorimager.

Labelling with biotin–streptavidin–nanogold. The central strand of DAE-O **B** was synthesized containing a 5′ biotin group. Lattices were formed by annealing as described. After annealing, a stoichiometric amount of streptavidin–nanogold (1.4 nm; Nanoprobe) in a buffer provided by the supplier (20 mM phosphate, 150 mM NaCl (pH 7.4), 0.1% BSA, 0.05% NaN_3) was added, so that the molar ratio of biotin to streptavidin was 1:1. The solution was left at room temperature for 1 h and then imaged by AFM as described below.

Preparation of AFM sample. 2–10 μl were spotted onto freshly cleaved mica (Ted Pella) and left to adsorb to the surface for 2 min. To remove buffer salts, 5–10 drops of doubly distilled or nanopure H_2O were placed on the mica, the drop was shaken off and the sample was dried with compressed air. Imaging was done under isopropanol in a fluid cell on a NanoScope II using the D or E scanner and commercial 200-μm cantilevers with Si_3N_4 tips (Digital Instruments). The feedback setpoint was adjusted frequently to minimize contact force to ~1 to 5 nN. Images were processed with a first- or third-order 'flatten filter', which independently subtracts a first- or third-order polynomial

fit from each scanline to remove tip artefacts; however, this technique can introduce false 'shadows'.

1. Liu, B., Leontis, N. B. & Seeman, N. C. Bulged 3-arm DNA branched junctions as components for nanoconstruction. *Nanobiology* **3**, 177–188 (1994).
2. Seeman, N. C. Nucleic-acid junctions and lattices. *J. Theor. Biol.* **99**, 237–247 (1982).
3. Cohen, S. N., Chang, A. C. Y., Boyer, H. W. & Helling, R. B. Construction of biologically functional bacterial plasmids *in vitro*. *Proc. Natl Acad. Sci. USA* **70**, 3240–3244 (1973).
4. Qiu, H., Dewan, J. & Seeman, N. C. A DNA decamer with a sticky end: The crystal structure of d-CGACGATCGT. *J. Mol. Biol.* **267**, 881–898 (1997).
5. Ma, R.-I., Kallenbach, N. R., Sheardy, R. D., Petrillo, M. L. & Seeman, N. C. Three-arm nucleic acid junctions are flexible. *Nucleic Acids Res.* **14**, 9745–9753 (1986).
6. Petrillo, M. L. *et al*. The ligation and flexibility of four-arm DNA junctions. *Biopolymers* **27**, 1337–1352 (1988).
7. Fu, T.-J. & Seeman, N. C. DNA double-crossover molecules. *Biochemistry* **32**, 3211–3220 (1993).
8. Schwacha, A. & Kleckner, N. Identification of double Holliday junctions as intermediates in meiotic recombination. *Cell* **83**, 783–791 (1995).
9. Li, X., Yang, X., Qi, J. & Seeman, N. C. Antiparallel DNA double crossover molecules as components for nanoconstruction. *J. Am. Chem. Soc.* **118**, 6131–6140 (1996).
10. Winfree, E. in *DNA Based Computers: Proceedings of a DIMACS Workshop, April 4, 1995, Princeton University* (eds Lipton, R. J. & Baum, E. B.) 199–221 (American Mathematical Society, Providence, RI, 1996).
11. Adleman, L. M. Molecular computation of solutions to combinatorial problems. *Science* **266**, 1021–1024 (1994).
12. Grünbaum, B. & Shephard, G. C. *Tilings and Patterns* (Freeman, New York, 1986).
13. Wang, H. in *Proc. Symp. Math. Theory of Automata* 23–56 (Polytechnic, New York, 1963).
14. Winfree, E., Yang, X. & Seeman, N. C. in *Proceedings of the 2nd DIMACS Meeting on DNA Based Computers, Princeton University, June 20–12, 1996* (American Mathematical Society, Providence, RI, in the press).
15. Reif, J. in *Proceedings of the 3rd DIMACS Meeting on DNA Based Computers, University of Pennsylvania, June 23–25, 1997* (American Mathematical Society, Providence, RI, in the press).
16. Binnig, G., Quate, C. F. & Gerber, C. Atomic force microscope. *Phys. Rev. Lett.* **56**, 930–933 (1986).
17. Wang, J. C. Helical repeat of DNA in solution. *Proc. Natl Acad. Sci. USA* **76**, 200–203 (1979).
18. Rhodes, D. & Klug, A. Helical periodicity of DNA determined by enzyme digestion. *Nature* **286**, 573–578 (1980).
19. Seeman, N. C. *De novo* design of sequences for nucleic acid structural engineering. *J. Biomol. Struct. Dyns* **8**, 573–581 (1990).
20. Yue, K. & Dill, K. A. Inverse protein folding problem—designing polymer sequences. *Proc. Natl Acad. Sci.* **89**, 4163–4167 (1992).
21. Sun, S., Brem, R., Chan, H. S. & Dill, K. A. Designing amino acid sequences to fold with good hydrophobic cores. *Prot. Engng* **9**, 1205–1213 (1996).
22. SantaLucia, J., Allawi, H. T. & Seneviratne, A. Improved nearest-neighbor parameters for predicting DNA duplex stability. *Biochemistry* **35**, 3555–3562 (1996).
23. Ouporov, I. V. & Leontis, N. B. Refinement of the solution structure of a branched DNA three-way junction. *Biophys. J.* **68**, 266–274 (1995).
24. Hansma, H. G. *et al*. Reproducible imaging and dissection of plasmid DNA under liquid with the atomic force microscope. *Science* **256**, 1180–1184 (1992).
25. Shaiu, W.-L., Larson, D. D., Vesenka, J. & Henderson, E. Atomic force microscopy of oriented linear DNA molecules labelled with 5 nm gold spheres. *Nucleic Acids Res.* **21**, 99–103 (1993).
26. Shaiu, W.-L., Vesenka, J., Jondle, D., Henderson, E. & Larson, D. D. Visualization of circular DNA molecules labelled with colloidal gold spheres using atomic force microscopy. *J. Vac. Sci. Tech. A* **11**, 820–823 (1993).
27. Whitesides, G. M., Mathias, J. P. & Seto, C. T. Molecular self-assembly and nanochemistry: a chemical strategy for the synthesis of nanostructures. *Science* **254**, 1312–1319 (1991).
28. Niemeyer, C. M., Sano, T., Smith, C. L. & Cantor, C. R. Oligonucleotide-directed self-assembly of proteins. *Nucleic Acids Res.* **22**, 5530–5539 (1994).
29. Alivisatos, A. P. *et al*. Organization of 'nanocrystal molecules' using DNA. *Nature* **382**, 609–611 (1996).
30. Mirkin, C. A., Letsinger, R. L., Mucic, R. C. & Storhoff, J. J. A DNA-based method for rationally assembling nanoparticles into macroscopic materials. *Nature* **382**, 607–609 (1996).
31. Braun, E., Eichen, Y., Sivan, U. & Ben-Yoseph, G. DNA-templated assembly and electrode attachment of a conducting silver wire. *Nature* **391**, 775–778 (1998).
32. Breaker, R. R. & Joyce, G. F. A DNA enzyme that cleaves RNA. *Chem. Biol.* **1**, 223–229 (1994).
33. Chen, J. & Seeman, N. C. The synthesis from DNA of a molecule with the connectivity of a cube. *Nature* **350**, 631–633 (1991).
34. Zhang, Y. & Seeman, N. C. The construction of a DNA truncated octahedron. *J. Am. Chem. Soc.* **116**, 1661–1669 (1994).
35. Joannopolous, J. D., Meade, R. D. & Winn, J. N. *Photonic Crystals: Moulding the Flow of Light* (Princeton University Press, Princeton, 1995).
36. Ribeiro, F. R. *et al*. Structure–activity relationships in zeolites. *J. Mol. Cat. A: Chem.* **96**, 245–270 (1996).
37. Robinson, B. H. & Seeman, N. C. The design of a biochip: A self-assembling molecular-scale memory device. *Prot. Engng* **1**, 295–300 (1987).
38. Haddon, R. C. & Lamola, A. A. The molecular electronic defice and the biochip computer: present status. *Proc. Natl Acad. Sci. USA* **82**, 1874–1878 (1985).
39. Carter, E. S. & Tung, C.-S. NAMOT2—a redesigned nucleic acid modelling tool: construction of non-canonical DNA structures. *CABIOS* **12**, 25–30 (1996).
40. Vainshtein, B. K. *Modern Crystallography, 1: Fundamentals of Crystals* (Springer, New York, 1994).